5-2-2019

Caspases and cancer: Connections through circular dichroism spectroscopy

Sarah M. Hethcox
Georgia Southern University

Caspases and cancer: Connections through circular dichroism spectroscopy

An Honors Thesis submitted in partial fulfillment of the requirements for Honors in the Department of Chemistry and Biochemistry

By
Sarah Madison Hethcox

Under the mentorship of Dr. C. Michele Davis McGibony

ABSTRACT

While excessive cell death inevitably leads to negative effects, the endurance of damaged cells in the presence of death signals can be equally detrimental to health. Apoptosis, or programmed cell death, is a highly regulated process in which cues from within or from outside a cell can trigger an irreversible sequence of signals that carry out cell destruction known as the apoptotic cascade. A group of enzymes called caspases play a vital role in this cascade with some participating as initiators and others acting as effectors of protein cleavage and intracellular breakdown. Although it is normal for the activity of caspases to be suppressed during a cell's lifetime, continued suppression of apoptotic enzymes even in the presence of pro-apoptotic signals is one of the hallmarks of cancer cells. There is evidence that certain metal ions can bind and inhibit caspases, and fluctuations in intracellular Fe^{3+} concentrations during apoptosis raise the question whether this ion has a similar effect. In this study, plasmid DNA encoding caspase-7 was expressed in *E. coli*, and the resulting protein was purified using nickel affinity chromatography. The protein's structure will be analyzed both on its own and in the presence of Fe^{3+} in order to determine whether interactions are present that may lead to caspase-7 inhibition. Structural changes will be monitored using circular dichroism spectroscopy. Further understanding of cationic interactions with caspases could answer many existing questions about apoptotic resistance in cells and perhaps even lead to the development of treatments for such conditions.

Thesis Mentor: _____

Dr. C. Michele Davis McGibony

Honors Director: _____

Dr. Steven Engel

April 2019
Department of Chemistry and Biochemistry
University Honors Program
Georgia Southern University

ACKNOWLEDGMENTS

I would like to express my gratitude to Dr. Michele McGibony for her guidance and encouragement throughout the duration of this project. Advice given by Dr. Amanda White has also been a great help in the planning and execution of this study. Finally, I wish to thank my colleagues Lauren Love and Zachary Chicosky for their help in the collection of my data and for their friendship along the way.

INTRODUCTION

Although disease is often thought of as damage to healthy cells, the lack of death in unneeded or unhealthy cells presents a host of complications of its own. The body relies on certain self-destructive processes to ensure that defective cells die off in a timely manner. These processes are kept in check under normal conditions, but cues from within or from outside a cell can trigger a sequence of signals and processes collectively known as the apoptotic cascade which ultimately brings about programmed cell death, also known as apoptosis. While apoptosis is necessary for development of tissues and for keeping those tissues healthy, excessive apoptosis can lead to degenerative diseases such as Alzheimer's disease, Huntington's disease, and Parkinson's disease,[1] while underactivity of apoptosis can lead to unregulated cell growth, which is characteristic of tumors and cancer.

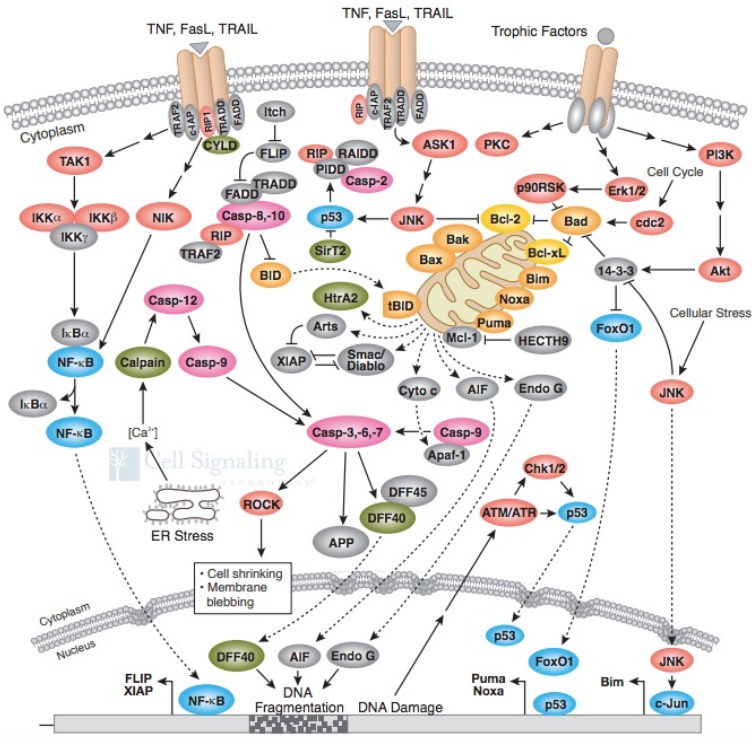

Figure 1. Apoptosis occurs in a complex and highly regulated cascade of processes in which enzymes called caspases (represented in pink) are central mediators.[2]

Apoptosis is a highly regulated process that is mediated by numerous different enzymes (Fig. 1), many of which lie dormant until acted upon by components higher up in the cascade. A group of cysteine proteases known as caspases play a vital role in this

cascade with some participating as initiators and others acting as effectors of protein cleavage and intracellular breakdown.[3] Procaspases, or caspases in their inactive zymogen form, can be activated through one of two main pathways (Fig. 2). The intrinsic pathway is activated by internal cellular stress caused by factors such as radiation, hypoxia, viral infection, or absence of necessary growth factors.[5] The extrinsic pathway involves signals from outside the cell such as the binding of tumor necrosis factor to transmembrane death receptors.[5] Once activated, caspases can be classified as initiators or executioners based on whether their function is to activate other caspases or to cleave and destroy other proteins throughout the cell.[3]

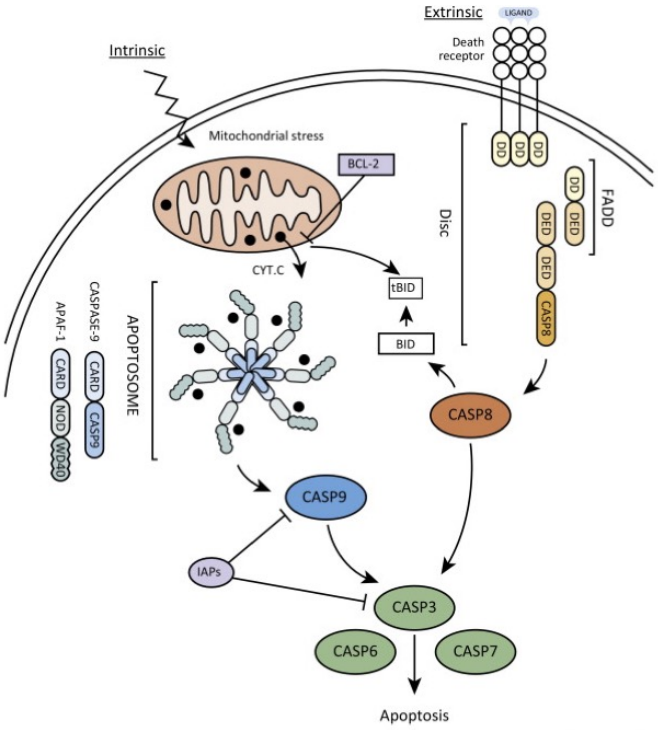

Figure 2. The intrinsic pathway of apoptosis (left) is initiated by intracellular stress while the extrinsic pathway (right) is elicited by extracellular death signals binding to transmembrane receptors.[4]

The focus of this study is executioner caspase-7. In its active form, caspase-7 exists as a tetramer composed of two identical heterodimers.[6] Each dimer is made up of two subunits (p10 and p20) with molecular weights of approximately 10 kDa and 20 kDa

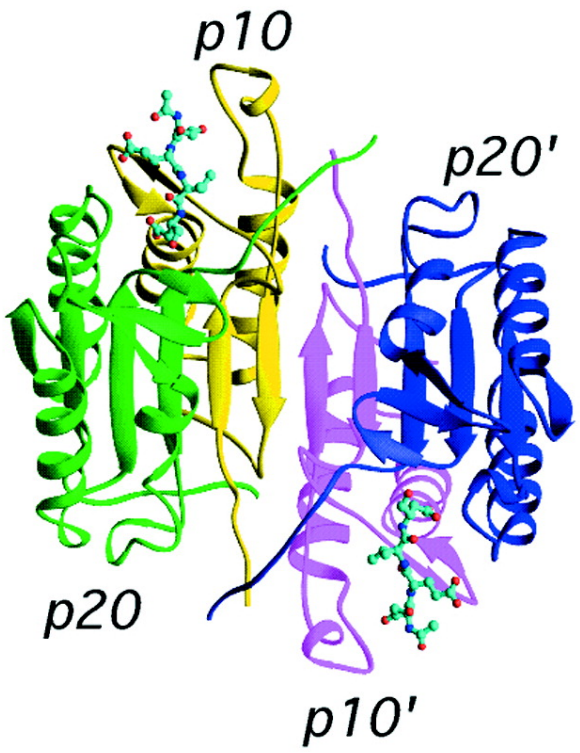

Figure 3. Above is the ribbon structure of tetrameric caspase-7 with its p10 and p20 subunits assembled with their symmetric equivalents, p10' and p20'. β sheets are represented as arrows, and α helices are shown as curled sections of the ribbon. Here the enzyme is bound to an inhibitor represented by the ball-and-stick structure.[6]

respectively.[6] As shown in Figure 3, the complete tetramer's structure is characterized by a central β sheet surrounded by ten α helices parallel to the β strands.[6] This structure is achieved by stabilization of individual zymogen dimers via cleavage of a linker that separates the p10 and p20 chains by initiator caspases (Fig. 4).[7]

Caspase-7 functions as an executioner caspase and is responsible for production of reactive oxygen species following mitochondrial outer membrane permeabilization (MOMP) and detachment of apoptotic cells from the extracellular matrix during apoptosis.[8] Caspase-7 also shares several substrates with caspase-3 including PARP, which plays a role in DNA repair[5,9] as well as ROCK I and α-fodrin, both of which are responsible for maintaining cytoskeleton shape.[10-12] Intrinsic activation of caspase-7 begins with intracellular stress leading to MOMP and the release of cytochrome c,

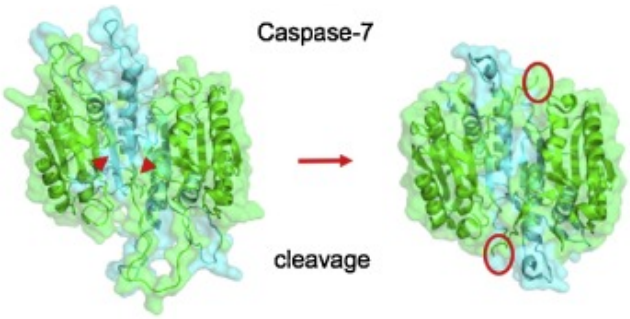

Figure 4. Procaspase-7 is activated by cleavage of inter-chain linkers (red arrowheads) by initiator caspases, resulting in stabilizing rearrangement of the active site (red circles).[7]

which contributes to the activation of caspase-9, an initiator caspase that goes on to activate executioners such as caspase-7.[8]

There are a few inhibitors of caspase-7 that are already well-known. These include proteins of the inhibitor of apoptosis (IAP) family which competitively inhibit substrate binding as well as p35 protein, which originates from a virus and inserts itself into the caspase's active site.[13] It has been shown that several of the caspases, including caspase-7, interact with and are inhibited by transition metal ions such as zinc(II) and copper(II).[14] Evidence that cancer cells are characterized by heightened dependence on intracellular iron[15] raises the question of whether iron(III) may be another metal ion that inhibits caspase activity by interference with the protein's structure.

In order to determine whether caspase-7 interacts with Fe^{3+} the protein was monitored for conformational change via circular dichroism (CD) spectroscopy, which is a well-established method for determining protein secondary structure (Fig. 5).[16] In this form of spectroscopic analysis, a plane of alternating left- and right-handed circularly polarized light is passed through an optically active sample such as a protein sample.[17] The resulting CD spectrum is a plot of the difference in absorbance of left- and right-handed circularly polarized light.[16]

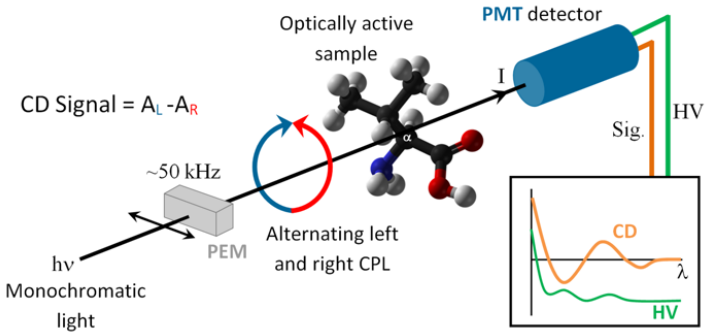

Figure 5. Circular dichroism (CD) involves passing a plane of alternating left- and right-handed circularly polarized light (CPL) through a protein sample and measuring the difference in their absorbances. Maxima and minima at specific wavelengths in the specrum are characteristic of certain secondary structure elements such as β sheets and α helices.[17]

Early attempts to analyze commercially produced caspase-7 resulted in noisy, unreliable CD spectra due to the glycerol storage buffer's absorbance in the wavelength region of interest.[16] However, dialysis left samples too dilute to obtain adequate CD spectra. Due to costliness and miniscule quantity-size of commercial caspase samples, it was decided that caspase-7 would be expressed and isolated in-house for this study.

MATERIALS AND METHODS

Caspase-7 was expressed, isolated, and analyzed using the techniques outlined in Figure 6 below.

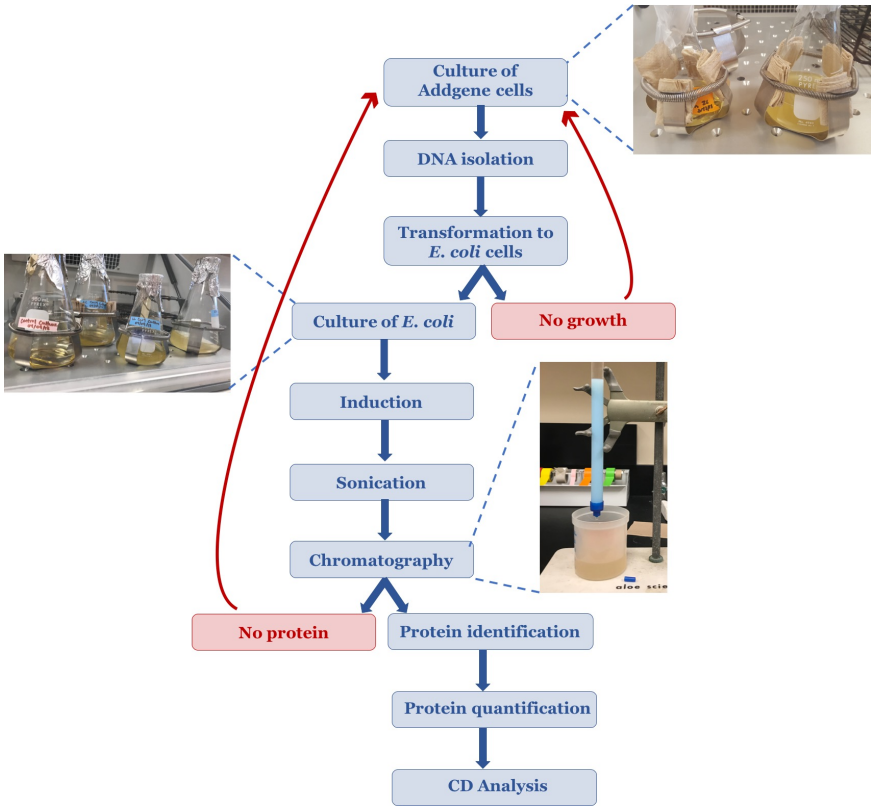

Figure 6. The flow chart above provides an overview of the experimental methods used in this study including isolation of commercial Addgene plasmids from host cells, transformation of those plasmids to *E. coli* DE3 cells, culture and induction of cells, lysis by sonication, protein purification by nickel affinity chromatography, protein identification via SDS-PAGE, protein quantification via Bradford assay, and finally structural analysis via CD spectroscopy.

DNA Isolation

Bacterial stab cultures containing plasmid DNA coding for caspase-7 with a histidine tag, specifically pET23b-Casp7-His (Addgene plasmid #11825) [18] were used to streak bacteria onto a Luria Broth (LB) Agar plate made with 100 µg/mL ampicillin. Single colonies were isolated and used to inoculate a 250 mL overnight culture of liquid LB with 100 µg/mL ampicillin, and the culture was allowed to grow at 200 rpm and 37°C in a shaking incubator (Fig. 7) until an OD_{600} of 0.7 was reached. The culture was then centrifuged at 5000 rpm for 20 minutes, and the supernatant was carefully discarded. The remaining bacterial pellet was then resuspended in minimal volume (about 10 mL) of cold buffer consisting of 25 mM Tris-HCl, 50 mM glucose, 10 mM EDTA, pH = 8. Twice the cell suspension's volume of denaturing solution (0.2 N NaOH, 1.0% SDS) was added, and the mixture was slowly inverted several times until the contents became clearer and thicker. The sample was then incubated on ice for 5 minutes. Next, about 1.5x the original cell suspension volume of cold renaturing solution (120 mL 5M potassium acetate, 23 mL glacial acetic acid, 57 mL dH_2O). The sample was mixed by inverting several times until a white precipitate formed containing bacterial proteins and genomic DNA (i.e. unwanted materials). The solution was incubated on ice for an additional 5 minutes, then centrifuged at 12,000 rpm for 5 minutes. The plasmid-containing supernatant was collected and treated with 2-2.5x the

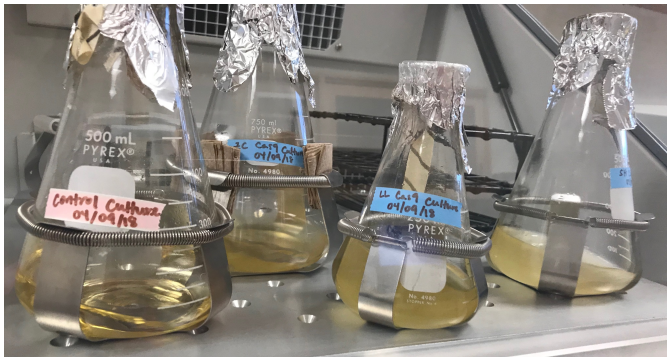

Figure 7. Shaking incubator holding bacterial cell cultures (three rightmost flasks) with visible growth characterized by cloudiness in comparison to the clear negative control (leftmost flask)

original cell suspension volume of cold 100% ethanol. This mixture was incubated at -20°C, uncapped, overnight. Upon thawing, the supernatant was discarded, and the pellet was allowed to air dry for 30 minutes. Finally, the pellet was resuspended in minimal TE buffer (10 mM Tris-HCl, 0.1 mM EDTA, pH = 8).

Protein Expression and Extraction

The plasmid DNA obtained with the Miniprep Kit was then transformed into BL21(DE3) *E. coli* cells[19] for expression of caspase-7 with a histidine tag. Following a protocol published by MilliporeSigma,[20] 1.00 µL of purified plasma DNA was added to a 25.0 µL aliquot of DE3 cell suspension. Transformation was initiated by incubation on ice for 5 minutes followed by heat shock in a 42°C water bath for 30 seconds. The sample was placed back on ice for an additional two minutes. Next, 250.0 µL of room temperature Super Optimal broth with Catabolite repression (SOC) medium was added to the sample, and the culture was allowed to grow at 37°C while shaking at 250 rpm for one hour. The transform was then poured and spread onto an LB agar plate made with 100 µg/mL ampicillin and incubated overnight at 37°C.

Next, 1 L of LB with 100 µL/mL ampicillin was inoculated with single colonies of DE3 cells containing caspase DNA from the transformation. This culture was allowed to grow at 37°C and shaking at 200 rpm until an OD_{600} of 0.7 was reached. The DE3 culture was then induced to generate caspase-7 by addition of 0.187 g isopropyl ß-D-1-thiogalactropyranoside (IPTG) to yield a final IPTG concentration of 0.8 mM. The temperature was reduced to 25°C, and the culture was allowed to grow for five hours. Cells were collected in pellets by centrifugation at 5000 rpm for twenty minutes.

The cells were resuspended in a minimal volume of low imidazole buffer consisting of 50 mM NaCl, 50 mM tris base, and 50 mM imidazole at pH = 7.9. The DE3 cells were lysed to release caspase-7 protein from cellular components by sonication, or agitation of the sample using sound waves. During sonication, the vibration of the sonicator probe tended to heat the cell suspension, so care was taken to sonicate in short pulses while keeping the sample on ice to prevent protein denaturation. The total sonication time was 30 minutes excluding rest time. The suspension was centrifuged at 14,000 rpm for 30 minutes to pellet unwanted cellular materials. The protein-rich supernatant was retained for purification.

Protein Purification

The cell lysate was applied to a chromatography column charged with nickel ions (Fig. 8) that would interact with the protein's histidine tag for isolation of caspase-7 by affinity chromatography. The loading wash was collected for SDS-PAGE analysis, and the column was washed with about 5x the resin bed volume of low imidazole buffer until absorbance at 280 nm showed that protein was no longer present in the wash. Three column washes of 75 mL were collected and retained for SDS-PAGE analysis. Finally, the desired caspase-7 protein was eluted from the column with about 2x the bed volume of high imidazole buffer consisting of 50 mM NaCl, 50 mM tris base, and 500 mM imidazole at pH = 7.9. The eluent was collected in 3 mL fractions, and the absorbance of

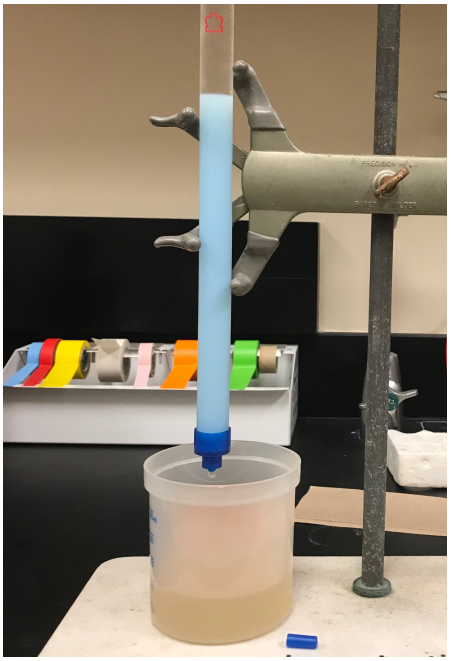

Figure 8. The chromatography column is characterized by blue color due to nickel(II) ions complexed to the resin for interaction with the histidine tag on caspase-7 proteins.

each was measured at 280 nm using a NanoDrop 2000c UV-Vis spectrophotometer to monitor the presence of protein in the fractions (Fig. 9). A full absorbance spectrum in the UV range from 200-400 nm was also conducted (Fig. 10).

Because imidazole and Cl^- ions interfere with CD spectroscopy signals, the protein-containing fractions were pooled and dialyzed using Spectra/Por® dialysis tubing with a molecular weight cutoff of 3.5 kDa. The protein sample was dialyzed overnight in a 1:20 volume ratio of sample to buffer (50 mM tris base, pH = 7.9), and a protease inhibitor, 4-benzenesulfonyl fluoride hydrochloride (AEBSF), was added to yield a final concentration of 0.27 mM.

Protein Identification

In order to confirm that the protein eluted from the chromatography column was in fact caspase-7, an SDS-PAGE gel was run using a low molecular weight ladder from Thermo Scientific (Product# 26612).[21] Samples from the pooled protein-containing chromatography fractions and from the first column wash were treated with a sample prep mix consisting of 7.5% 2-mercaptoethanol, 7.5% SDS, 0.05% bromphenol blue, 25% glycerol and boiled to denature the proteins. A 12.5% polyacrylamide gel was submerged in 1x EZ Run buffer, loaded with samples and ladder, and run at 150 V for

about 1.5 hours. The gel was stained for one hour with 0.1% Coomassie Brilliant Blue R-250, 40% methanol, 10% acetic acid, then destained overnight with 40% methanol, 10% acetic acid (Fig. 11). The distances traveled by bands in the ladder were measured and plotted versus the log of the molecular weights corresponding with each band[21] to produce a linear regression (Fig. 12) to be used for analysis of sample molecular weights.

Protein Quantification

A Bradford protein assay[22] was performed in order to quantify the amount of caspase-7 obtained during the purification process. Standard solutions of bovine serum albumin (BSA) at ten different concentrations from 0.10 to 1.00 mg/mL along with samples of the caspase-7 pooled fractions and a 1:2 dilution of the caspase-7 pooled fractions were treated with Bradford reagent. Their absorbances were then measured at 595 nm using a NanoDrop 2000c UV-Vis spectrophotometer. The concentrations of the caspase-7 samples were calculated using the linear equation produced by plotting the absorbances of the BSA standards at 595 nm versus their corresponding concentrations (Fig. 13). These results were averaged to obtain a concentration of the stock caspase-7 solution (Table 2).

CD Analysis of Caspase-7

A sample of dialyzed caspase-7 was diluted with tris buffer, pH = 7.9, to a yield final protein concentration of 0.1 mg/mL. This sample was analyzed using a JASCO J-815 CD Spectrophotometer in order to obtain a baseline scan for the isolated protein's secondary structure (Fig. 14). In order to monitor any changes in the protein's secondary

structure due to interaction with Fe^{3+} ions, a 3.23 mM stock solution of iron(III) nitrate nonahydrate was created such that addition of Fe^{3+} solution by the microliter would yield a 1:1 mole-to-mole ratio of caspase-7 to Fe^{3+}. The caspase-7 sample will next be treated with 1.00 µL iron stock and analyzed via CD. This will be repeated three times, taking CD scans with each consecutive iron treatment, until a caspase-7 to Fe^{3+} mole ratio of 1:4 is reached.

RESULTS

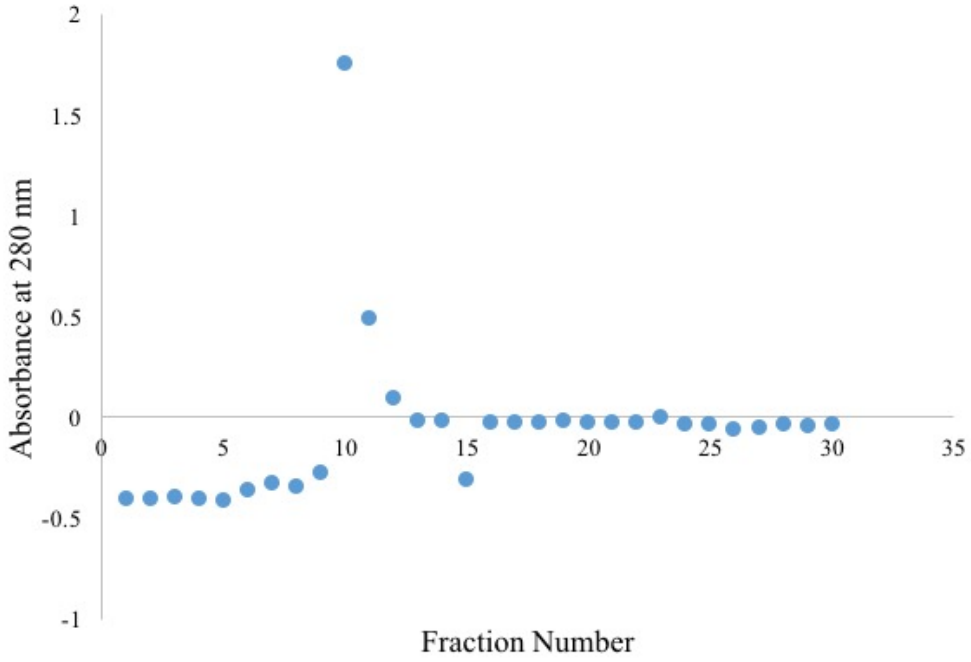

Figure 9. Elution profile of absorbance at 280 nm versus fraction number during elution of protein from nickel affinity chromatography column.

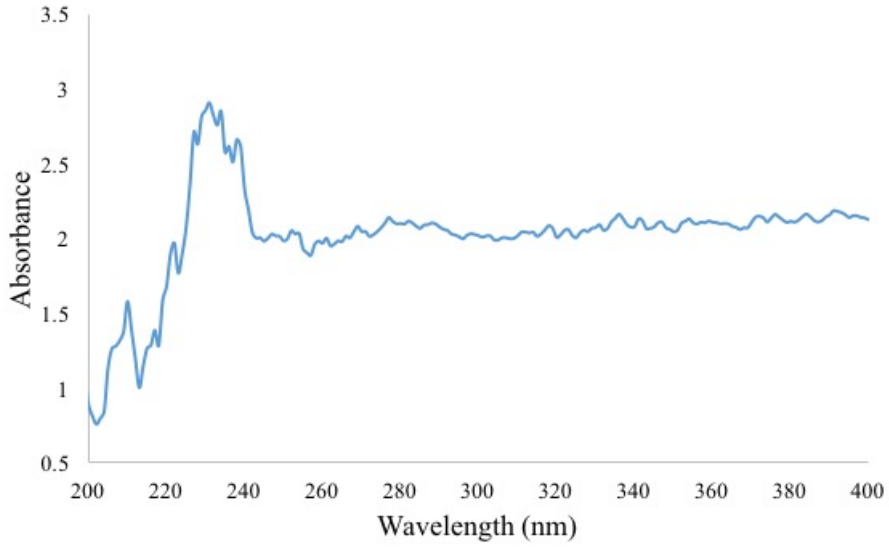

Figure 10. Full absorbance spectrum in the UV range of 200-400 nm for caspase-7 pooled fractions.

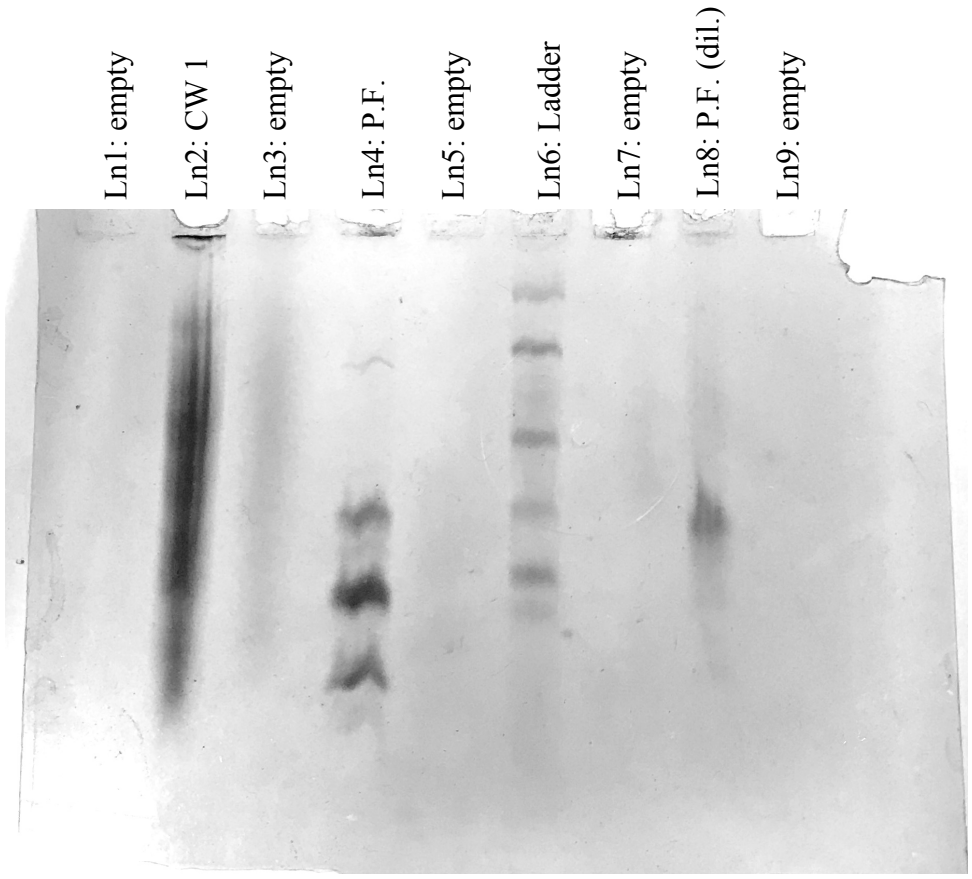

Figure 11. Image of 12.5% polyacrylamide gel from SDS-PAGE performed on column wash 1 (lane 2), pooled fractions (lane 4), standard MW ladder (lane 6), and pooled fractions diluted 1:2 (lane 8).

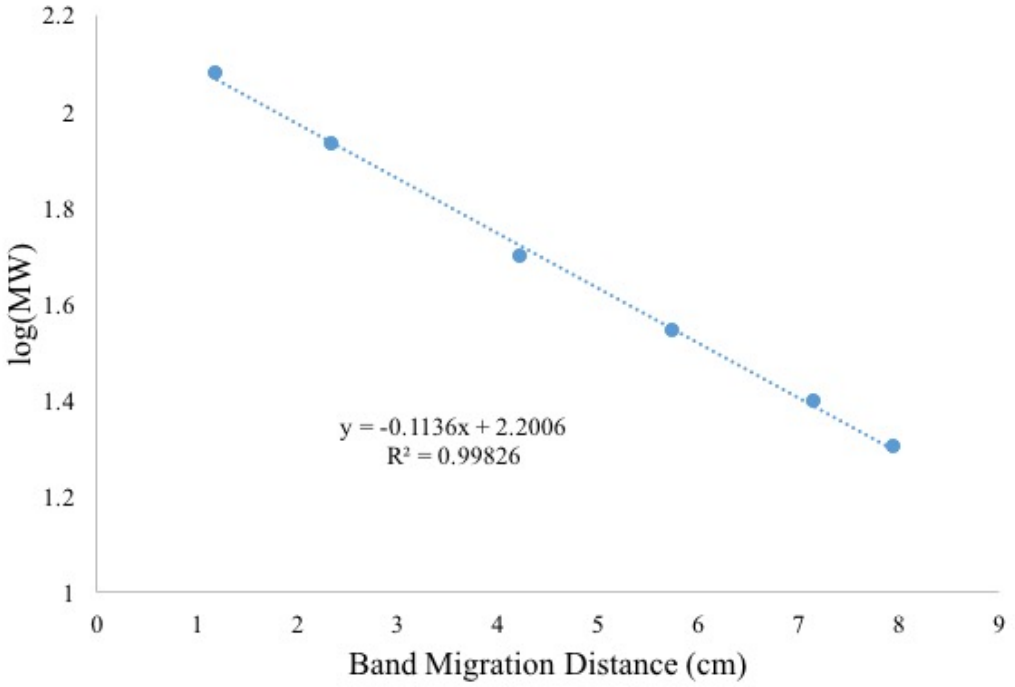

Figure 12. Standard curve of the logarithm of molecular weight in kilodaltons vs. band migration distance in centimeters for the MW ladder in the SDS-PAGE gel shown in Figure 5 along with the linear equation of best fit and its corresponding R^2 generated by Excel.

Table 1. Calculated molecular weights of bands in lane 4 (pooled fractions) from SDS-PAGE.

Band	Band Migration Distance (cm)	log(MW)	MW (kDa)
P.F. Band 1	5.93	1.527	33.6
P.F. Band 2	7.60	1.337	21.7
P.F. Band 3	9.35	1.138	13.8

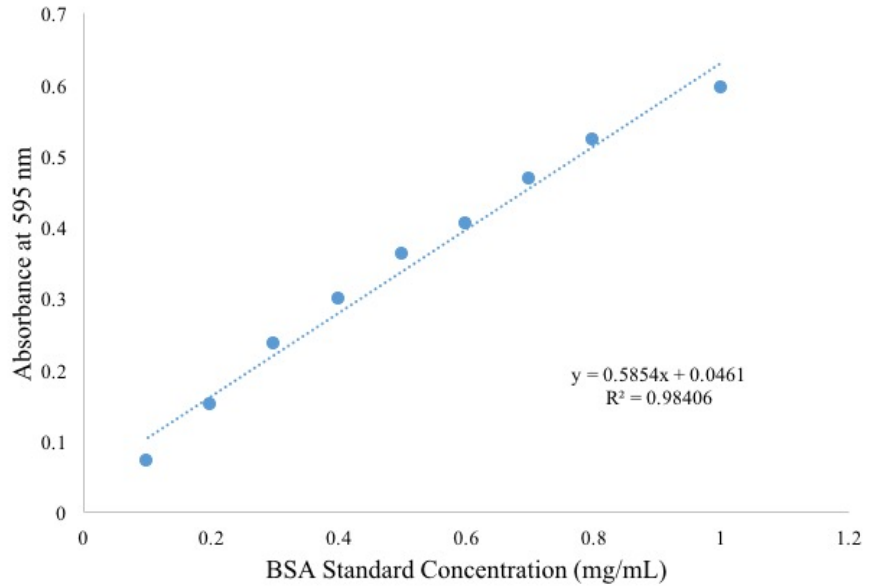

Figure 13. Bradford assay standard curve of absorbance at 595 nm versus BSA concentration (mg/mL) along with the linear equation of best fit and its corresponding R^2 generated by Excel.

Table 2. Summary of results from Bradford protein assay which determined the concentration and total protein content of the caspase-7 stock solution following dialysis.

Sample	Abs_{595}	Concentration (mg/mL)
Cas-7 (stock)	0.662	1.05
Cas-7 (1:2 dilution)	0.347	0.514

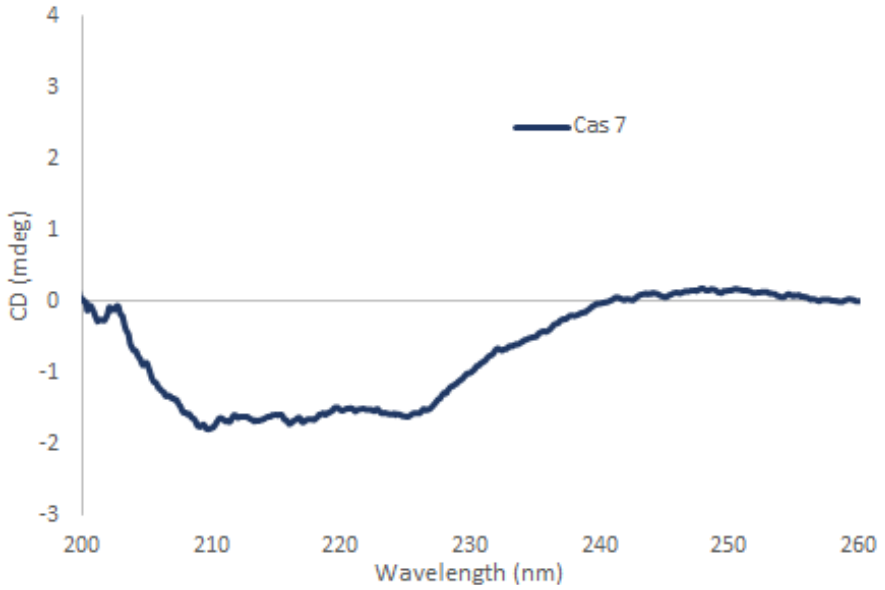

Figure 14. CD spectrum of isolated caspase-7 in tris buffer solution.

DISCUSSION

The method of purification used following protein expression and extraction was nickel affinity chromatography. When the column was loaded, the histidine tag on caspase-7 interacted with the nickel ions embedded in the resin, and all unwanted proteins and bacterial components were washed from the column with low imidazole buffer. Since the presence of amino acids with aromatic side chains causes proteins to absorb 280 nm light, the presence of protein in the column wash was monitored via UV-Vis spectroscopy. Once no more protein was detected in the column wash, the supposed caspase-7 was eluted from the column by washing with a buffer fairly concentrated with imidazole, which effectively displaced the proteins' histidine tags from the resin and allowed caspase-7 to wash from the column. As shown in Figure 9, the absorbance values shown in the elution profile are initially negative due to blanking with high imidazole buffer and initial rinsing of low imidazole buffer from the column. The peak in absorbance that occurs from fraction 10 to fraction 12 reflects the elution of protein from the column.

Following purification, samples from the eluent obtained were denatured and analyzed via SDS-PAGE as shown in Figure 11. This form of gel electrophoresis separates protein chains by molecular weight (i.e. smaller chains migrate farther while larger chains are more impeded by the gel polymers and migrate shorter distances). After the migration distances of each band from its well was measured (Fig. 11), the linear plot of log(MW) vs. band migration distance shown in Figure 12 was created. The resulting R^2 value of 0.998 points to the linear equation's validity.

As shown in Figure 11, lane 2 contains the column wash (i.e. bacterial proteins and unwanted material that washed through the column without interacting with the nickel ligands) and appears as a smear due to the presence of countless proteins of different molecular weights. The sample of interest is pooled fractions containing the eluted protein (lane 4). As expected, distinct bands appeared indicating the presence of purified polypeptide chains. By inserting measured distances of the pooled fraction bands into the linear equation from Figure 12 and solving for MW, the following results were obtained: In lane 4, the band that traveled shortest distance (P.F. Band 1) is 33.6 kDa, the middle band (P.F. Band 2) is 21.7 kDa, and the band that traveled the farthest (P.F. Band 3) is 13.8 kDa (Table 1). In lane 8, the single band is 33.0 kDa. Results for Bands 2 and 3 agree with literature values for the subunit molecular weights stated previously.[6] As such, one may conclude that these correspond with the two different subunits while Band 3 corresponds with the intact heterodimer.

Following identification of the protein via SDS-PAGE, the amount of caspase-7 isolated was quantified by the Bradford protein assay. The reagent dye used in this assay exists in its deprotonated form when it interacts with protein, and this form of the dye absorbs 595 nm light.[22] Therefore, absorbance at 595 nm can be directly related to protein concentration by creating a standard curve as shown in Figure 13. Caspase-7 concentration in the pooled fraction was determined by evaluating the standard curve's linear equation for concentration based on observed absorbance values (Table 2). After accounting for the twofold dilution factor in the P.F. (diluted) result, the concentrations obtained can be averaged to obtain a mean caspase-7 concentration of 1.04 mg/mL. With a total volume of 10.9 mL, this means that 11.3 mg of caspase-7 were collected in total.

The baseline CD scan for caspase-7 shown in Figure 14 is promising because it contains certain expected elements. Minima at 208 nm and 222 nm are characteristic of α-helical structure,[16] which caspase-7 is known to contain (Fig. 3).[6] This serves as additional evidence of the successful expression and purification of caspase-7. However, while attempting to analyze caspase-7 treated with Fe^{3+}, the CD spectrophotometer malfunctioned, and the issues were not resolved in time for final results to be included in this work.

CONCLUSION

This study was successful in the expression, purification, and quantification of caspase-7. Insight into the protein's secondary structure through CD spectroscopy was also accomplished. However, CD results for caspase-7 treated with Fe^{3+} are still pending, and any protein-ion interactions have yet to be determined. If further analysis via CD spectroscopy indicates that caspase-7 does undergo a conformational change in the presence of Fe^{3+}, future studies would include activity assays to determine whether any observed conformational changes are accompanied by decreased enzyme function. Additionally, isothermal titration calorimetry could be performed in order to calculate the caspase's binding affinity for Fe^{3+}, if any. The overarching project, of which this study is merely a small part, aims to study a variety of caspases, including initiator caspases-8 and -9 as well as executioner caspases-3 and -6, and their interactions with other biologically active metal ions such as Fe^{2+} and Ca^{2+}. Further understanding of caspases and their interactions could very well lead to the treatment and/or prevention of conditions resulting from dysregulation of apoptosis.

REFERENCES

1. Xu, X.; Lai, Y.; Hua, Z.C. Apoptosis and apoptotic body: disease message and therapeutic target potentials. *Biosci. Rep.* [Online] **2019,** *39* (1) DOI: 10.1042/BSR20180992. http://www.bioscirep.org/content/39/1/BSR20180992 (accessed Apr 20, 2019).

2. Cell Signaling Technology. Regulation of Apoptosis: Interactive Pathway. https://www.cellsignal.com/contents/science-cst-pathways-apoptosis/regulation-of-apoptosis-interactive-pathway/pathways-apoptosis-regulation (accessed Apr 20, 2019).

3. Thornberry, N.A. and Lazebnik, Y. Caspases: Enemies Within. *Science (Washington, DC, U.S.)* [Online] **1998,** *281*, 1312-1316 https://www.jstor.org/stable/2896430 (accessed Oct 23, 2018).

4. Creagh, E. M. Caspase crosstalk: integration of apoptotic and innate immune signaling pathways. *Trends Immunol.* [Online] **2014,** *35*(12), 631-640. DOI: 10.1016/j.it.2014.10.004. https://www.cell.com/trends/immunology/fulltext/S1471-4906(14)00189-6?_returnURL=https%3A%2F%2Flinkinghub.elsevier.com%2Fretrieve%2Fpii%2FS1471490614001896%3Fshowall%3Dtrue (accessed Oct 21, 2017).

5. Elmore, S. Apoptosis: A Review of Programmed Cell Death. *Toxicol. Phathol.* [Online] **2007,** *35* (4), 495-516. National Center for Biotechnology Information. https://www.ncbi.nlm.nih.gov/pmc/articles/PMC2117903/ (accessed Nov 1, 2018).

6. Wei, Y.; Fox, T.; Chambers, S.P.; Sintchak, J.; Coll, J.T.; Golec, J.M.C.; Swenson, L.; Wilson, K.P.; Charifson, P.S. The structures of caspases-1, -3, -7 and -8 reveal the basis for substrate and inhibitor selectivity. *Chem. Biol. (Oxford, U. K.)* [Online] **2000,** *7*(6), 423-432. DOI: 10.1016/S1074-5521(00)00123-X. https://www.cell.com/cell-chemical-biology/fulltext/S1074-5521(00)00123-X?_returnURL=https%3A%2F%2Flinkinghub.elsevier.com%2Fretrieve%2Fpii%2FS107455210000123X%3Fshowall%3Dtrue (accessed Apr 20, 2019).

7. Gonzalez Ramirez, M.L. and Salvesen, G.S. A primer on caspase mechanisms. *Semin. Cell Dev. Biol.* [Online] **2018,** *82*, 79-85. ScienceDirect. https://www-sciencedirect-com.libez.lib.georgiasouthern.edu/science/article/pii/S1084952117301088#bib0065 (accessed Apr 20, 2019).

8. Brentnall, M.; Rodriguez-Menocal, L.; De Guevara, R.L.; Cepero, E.; Boise, L.H. Caspase-9, -3, and -7 have distinct roles during intrinsic apoptosis. *BMC Cell Biol.* [Online] **2013**, *14* (32) http://www.biomedcentral.com/1471-2121/14/32 (accessed Oct 22, 2018).

9. Slee, E. A.; Adrian, C.; Martin, S.J. Executioner Caspase-3, -6, and -7 Perform Distinct, Non-redundant Roles during the Demolition Phase of Apoptosis. *J. Biol. Chem.* [Online] **2000,** *276*, 7320-7326 http://www.jbc.org/content/276/10/7320.long (accessed Nov 1, 2018).

10. Boucher, D.; Blais, V.; Denault, J.B. Caspase-7 uses an exosite to promote poly(ADP ribose) polymerase 1 proteolysis. *Proc. Natl. Acad. Sci. USA* [Online] **2012,** *109* (15), 5669-5674. National Center for Biotechnology Information. https://www.ncbi.nlm.nih.gov/pmc/articles/PMC3326497/ (accessed Nov 1, 2018).

11. Liao, J.K.; Seto, M.; Noma, K. Rho Kinase (ROCK) Inhibitors. *J. Cardiovasc. Pharmacol.* [Online] **2007,** *50* (1), 17-24. National Center for Biotechnology Information. https://www.ncbi.nlm.nih.gov/pmc/articles/PMC2692906/ (accessed Nov 1, 2018).

12. Hu, Q.; Wang, D.; Chen, W. The accuracy of the anti-α-fodrin antibody test for diagnosis of Sjogren's syndrome: A meta-analysis. *Clin. Biochem.* [Online] **2013,** *46* (15), 1372-1376. ScienceDirect. https://www.sciencedirect.com/science/article/pii/S0009912013001604?via%3Dihub (accessed Nov 1, 2018).

13. Shi, Y. Mechanisms of Caspase Activation and Inhibition during Apoptosis. *Mol. Cell* [Online] **2002,** *9* (3), 459-470 DOI: 10.1016/S1097-2765(02)00482-3. https://www.cell.com/molecular-cell/fulltext/S1097-2765(02)00482-3?_returnURL=https%3A%2F%2Flinkinghub.elsevier.com%2Fretrieve%2Fpii%2FS1097276502004823%3Fshowall%3Dtrue (accessed Nov 1, 2018).

14. Valazquez-Delgado, E.M. and Hardy, J.A. Zinc-mediated Allosteric Inhibition of Caspase-6. *J. Biol. Chem.* [Online] **2012,** *287*, 36000-36011. National Center for Biotechnology Information. https://www.ncbi.nlm.nih.gov/pmc/articles/PMC3476268/ (accessed Nov 1, 2018).

15. Manz, D.H.; Blanchette, N.L.; Bibbin, T.P.; Torti, F.M.; Torti, S.V. Iron and cancer: recent insights. *Ann. N.Y. Acad. Sci.* [Online] **2016,** *1368* (1), 149-161. National Center for Biotechnology Information. https://www.ncbi.nlm.nih.gov/pmc/articles/PMC4870095/ (accessed Apr 3, 2019).

16. Greenfield, N.J. Using circular dichroism spectra to estimate protein secondary structure. *Nat. Protoc.* [Online] **2006,** *1* (6), 2876-2890. National Center for Biotechnology Information. https://www.ncbi.nlm.nih.gov/pmc/articles/PMC2728378/ (accessed Apr 3, 2019).

17. Aarhus University. ISA, Centre for Storage Ring Facilities. http://www.isa.au.dk/facilities/astrid2/beamlines/au-cd/AU-CD_3.asp (accessed Mar 27, 2019).

18. Zhou Q.; Snipas S.; Orth K.; Muzio M.; Dixit V.M.; Salvesen, G.S. Target protease specificity of the viral serpin CrmA. Analysis of five caspases. *J. Biol. Chem.* [Online] **1997,** *272* (12), 7797-800 http://www.jbc.org/content/272/12/7797.long (accessed Apr 3, 2019).

19. *BL21(DE3) Singles™ Competent Cells – Novagen.* MSDS No. RC0030 [Online]; EMD Biosciences, Inc.: Madison, WI. http://www.emdmillipore.com/Web-US-Site/en_CA/-/USD/ProcessMSDS-Start?PlainSKU=EMD_BIO-70235&Origin=PDP (accessed Apr 3, 2019).

20. pET System Manual, 11th Edition [Online]; Novagen®: Darmstadt, Germany. http://www.emdmillipore.com/Web-US-Site/en_CA/-/USD/ShowDocument-File?ProductSKU=EMD_BIO-70235&DocumentId=TB055.pdf&DocumentUID=746753&DocumentType=USP&Language=EN&Country=US&Origin=PDP (accessed Jan 31, 2019).

21. *Pierce™ Prestained Protein MW Marker*, MSDS No. 26612 [Online]; Life Technologies Corporation: Carlsbad, CA. https://www.thermofisher.com/document-connect/document-connect.html?url=https%3A%2F%2Fassets.thermofisher.com%2FTFS-Assets%2FLSG%2FSDS%2F26612_MTR-NALT_EN.pdf&title=MjY2MTI (accessed Apr 3, 2019).

22. McGibony, M. D. and Stewart, A. S. *Georgia Southern University Biochemistry I Laboratory Manual*; Department of Chemistry and Biochemistry: Statesboro, GA, 2017.